

N-Heterocyclic carbene-catalyzed enantioselective synthesis of planar-chiral cyclophanes via dynamic kinetic resolution

Received: 7 August 2023

Accepted: 23 February 2024

Published online: 15 March 2024

Check for updates

Jiayan Li^{1,4}, Ziyang Dong^{1,4}, Yang Chen², Zhanhui Yang², Xinen Yan¹, Meng Wang³, Chenyang Li³✉ & Changgui Zhao¹✉

Planar-chiral cyclophanes have gained considerable concerns for drug discovery due to their unique conformational strain and 3D structure. However, the enantioselective synthesis of planar-chiral cyclophanes is a long-standing challenge for the synthetic community. We herein describe an N-heterocyclic carbene (NHC)-catalyzed asymmetric construction of planar-chiral cyclophanes. This transformation occurs through a dynamic kinetic resolution (DKR) process to convert racemic substrates into planar-chiral macrocycle scaffolds in good to high yields with high to excellent enantioselectivities. The *ansa* chain length and aromatic ring substituent size is crucial to achieve the DKR approach. Controlled experiments and DFT calculations were performed to clarify the DKR process.

Macrocycles exhibit unique properties including shape diversity, conformational pre-organization, and conformational flexibility, compared to small-sized rings, particularly, five- to seven-membered rings^{1,2}. The large surface area and tunable conformation of macrocycles increase the likelihood that the macrocycle will make meaningful contact with a biological target^{1,3}. The compilation of macrocyclic small molecule screening libraries is critical to success when challenging, underexploited, or poorly “druggable” biological targets, such as lorlatinib, are involved^{1,4}. Cyclophanes, which are molecules with an aromatic scaffold bearing a cross-linked chain, also called an *ansa* chain, are a subset of macrocycles^{5–7}. Notably, cyclophane with a short *ansa* chain and bulky aromatic substituents exhibit planar chirality, which arises from the restricted bond flip of the aromatic ring^{8–10}. Although planar-chiral cyclophanes are part of small molecule screening collections, these compounds have been increasingly used in drug development^{11,12}, asymmetric synthesis¹³, and functional materials¹⁴ (Fig. 1A), and additional planar-chiral cyclophanes could benefit these collections. However, the enantioselective synthesis of planar-chiral cyclophanes represents a formidable challenge to the synthetic community and hampers their widespread inclusion in drug development efforts^{15,16}.

Historically, the asymmetric synthesis of cyclophanes relied on chiral pools and chiral auxiliaries^{17–21}. Asymmetric catalysis now provides access to the enantiopure planar-chiral cyclophanes¹⁶, as seen in Tanaka’s seminal asymmetric arene formation strategy to produce chiral metacyclophanes via rhodium-catalyzed alkyne cyclotrimerization²². Inspired by Tanaka’s pioneering work, several elegant enantioselective inter- and intramolecular [2 + 2 + 2] cycloaddition processes were reported for planar-chiral cyclophane assembly (Fig. 1B, I)^{23–25}. In addition, asymmetric macrocyclization strategies have also provided access to planar-chiral cyclophanes^{26–32}. Very recently, Collins²⁸, Yang²⁹, and Li³⁰ independently developed enzyme-, chiral phosphoric acid (CPA)- or Pd-catalyzed asymmetric macrocyclization to achieve planar-chiral macrocycles (Fig. 1B, II). In addition to these processes, the desymmetrization is also an attractive method to afford planar-chiral structures. Shibata achieved the enantioselective synthesis of planar-chiral cyclophanes by *ortho*-lithiation of the achiral cyclophanes (Fig. 1B, III)³³. The fourth is dynamic kinetic resolution (DKR) of achiral cyclophanes (Fig. 1B, IV). The challenges in generating planar-chiral cyclophanes by a DKR process involve identifying appropriately sized aromatic ring substituents and *ansa* chain lengths, which will allow rapid racemization of the substrate but limit the bond flip of the aromatic ring in the

¹Key Laboratory of Radiopharmaceuticals, Ministry of Education, College of Chemistry, Beijing Normal University, Beijing 100875, China. ²Department of Organic Chemistry, College of Chemistry, Beijing University of Chemical Technology, Beijing 100029, China. ³Key Laboratory of Theoretical and Computational Photochemistry, Ministry of Education, College of Chemistry, Beijing Normal University, Beijing 100875, China. ⁴These authors contributed equally: Jiayan Li, Ziyang Dong. ✉e-mail: chenyang.li@bnu.edu.cn; cgzhao@bnu.edu.cn

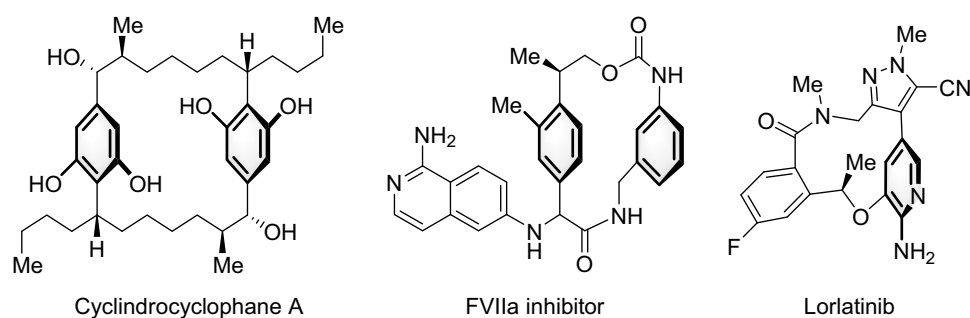
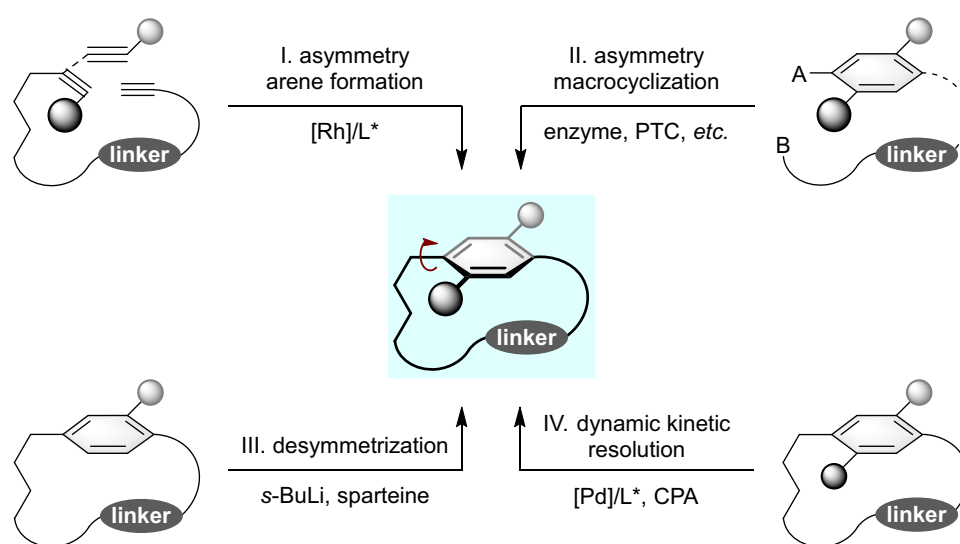
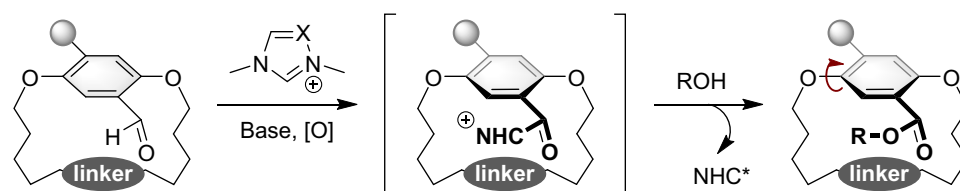
A Selected examples of molecules containing a planar-chiral cyclophane.**B** Approaches for the catalytic enantioselective synthesis of cyclophanes.**C** Design of an NHC-catalyzed enantioselective DKR of cyclophanes.**This design**

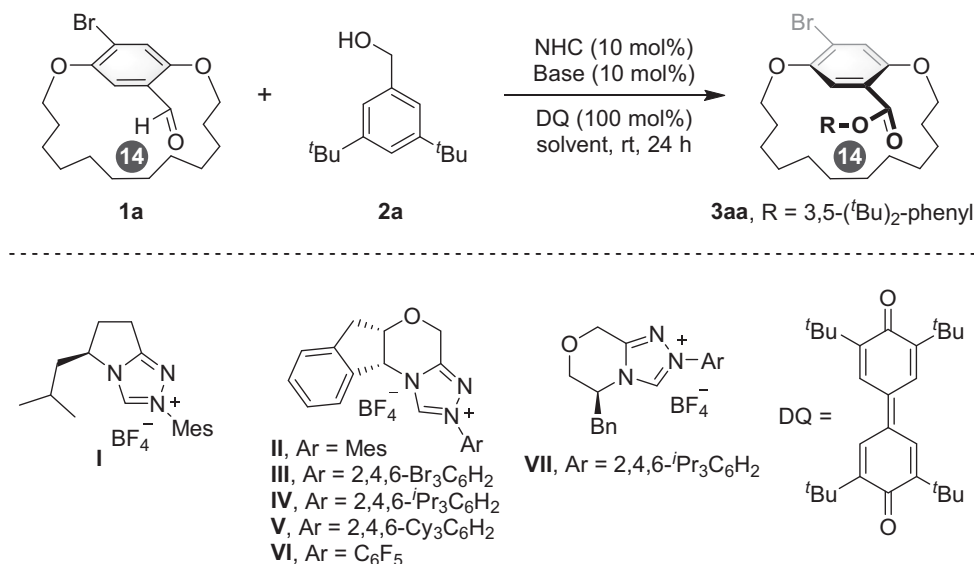
Fig. 1 | Importance of cyclophanes and the enantioselective synthesis. **A** Selected examples of molecules containing a planar-chiral cyclophane. **B** Approaches for the catalytic enantioselective synthesis of cyclophanes. **C** Design of an NHC-catalyzed enantioselective DKR of cyclophanes.

product. Both components are necessary to ensure the configurational stability of the resulting planar-chiral cyclophanes. In this scenario, Shibata was able to produce the chiral cyclophanes by a double asymmetric Sonogashira coupling of achiral $[n, n]$ paracyclophanes³⁴. More recently, Yang demonstrated an elegant CPA-catalyzed asymmetric electrophilic aromatic amination protocol to deliver planar-chiral macrocycles³⁵.

Despite the previously mentioned straightforward approaches to afford planar-chiral cyclophanes, limitations include variable

enantiomeric excess for different substrates, low reaction efficiencies, limited scope, and the use of stoichiometric amounts of chiral reagents. Further, the current protocols are restricted to a handful of catalytic models, and organocatalytic enantioselective synthetic routes are still in their infancy¹⁶. Consequently, these challenges prompted us to develop a DKR approach to achieve optically pure planar-chiral cyclophanes.

Chiral N-heterocyclic carbenes (NHCs) have been widely used as powerful organo-catalysts to access molecular architectures^{36–44}.



Entry ^a	NHC	Base	Solvent	Yield (%) ^b	er (%) ^c
1	I	DBU	THF	87	42:58
2	II	DBU	THF	97	64:36
3	III	DBU	THF	92	50:50
4	IV	DBU	THF	78	93:7
5	V	DBU	THF	70	93:7
6	VI	DBU	THF	90	65:35
7	VII	DBU	THF	80	16:84
8	IV	K ₂ CO ₃	THF	10	90:10
9	IV	Cs ₂ CO ₃	THF	69	93:7
10	IV	KO ^{<i>t</i>} Bu	THF	44	91:9
11	IV	DBU	EtOAc	61	87:13
12	IV	DBU	2-Me-THF	66	93:7
13	IV	DBU	MTBE	63	87:13
14 ^d	V	DBU	THF	76	93:7
15 ^e	V	DBU	THF	76	95:5

Fig. 2 | Optimization of the reaction conditions. ^aReaction conditions: A mixture of **1a** (0.10 mmol), **2a** (0.12 mmol), DQ (0.10 mmol), Base (10 mol%), and NHC catalyst (10 mol%) in solvent (2.0 mL) was stirred at room temperature for 24 h, the

number in the black circle is the *ansa* chain length. ^bIsolated yield. ^cDetermined by HPLC using a chiral stationary phase. ^dNHC catalyst (5 mol%); the reaction was stirred for 48 h. ^eThe reaction was performed at 40 °C.

However, most previous reports focused on the synthesis of central chirality, and more recently, axial chirality^{45–49}. Only recently has successful control of planar-chiral ferrocenes through NHC catalysis been reported by Chi⁵⁰. Herein, we disclose an NHC-catalyzed DKR of racemic cyclophanes by an oxidative esterification reaction to afford the planar-chiral cyclophanes in good to high yields with high to excellent enantioselectivities (Fig. 1C). We have also demonstrated that our enantioenriched products can be easily converted into diverse planar-chiral scaffolds for potential library inclusion and asymmetric catalysis through cross-coupling reactions. Controlled experiments and DFT calculations were performed to clarify the DKR process.

Results

Reaction optimization

We set out to explore the DKR of cyclophanes by examining the reaction of [14]paracyclophane **1a** with (3,5-*di-tert*-butylphenyl)methanol **2a** in the presence of triazolium NHC as catalyst (Fig. 2). The atropisomerism of **1a** was observed by variable temperature ¹H NMR experiments (below –50 °C), suggesting a low rotational energy barrier for [14]cyclophane **1a** at room temperature. Using 1,8-diazabicyclo[5.4.0]undec-7-ene (DBU) as base, 3,3',5,5'-tetratert-butylidiphenylquinone (DQ) as oxidant, and THF as solvent, various chiral triazolium NHC catalysts **I–VII** were initially screened (entries 1–7). The pyrrolotriazolium-derived NHC catalyst **I** exhibited high conversion

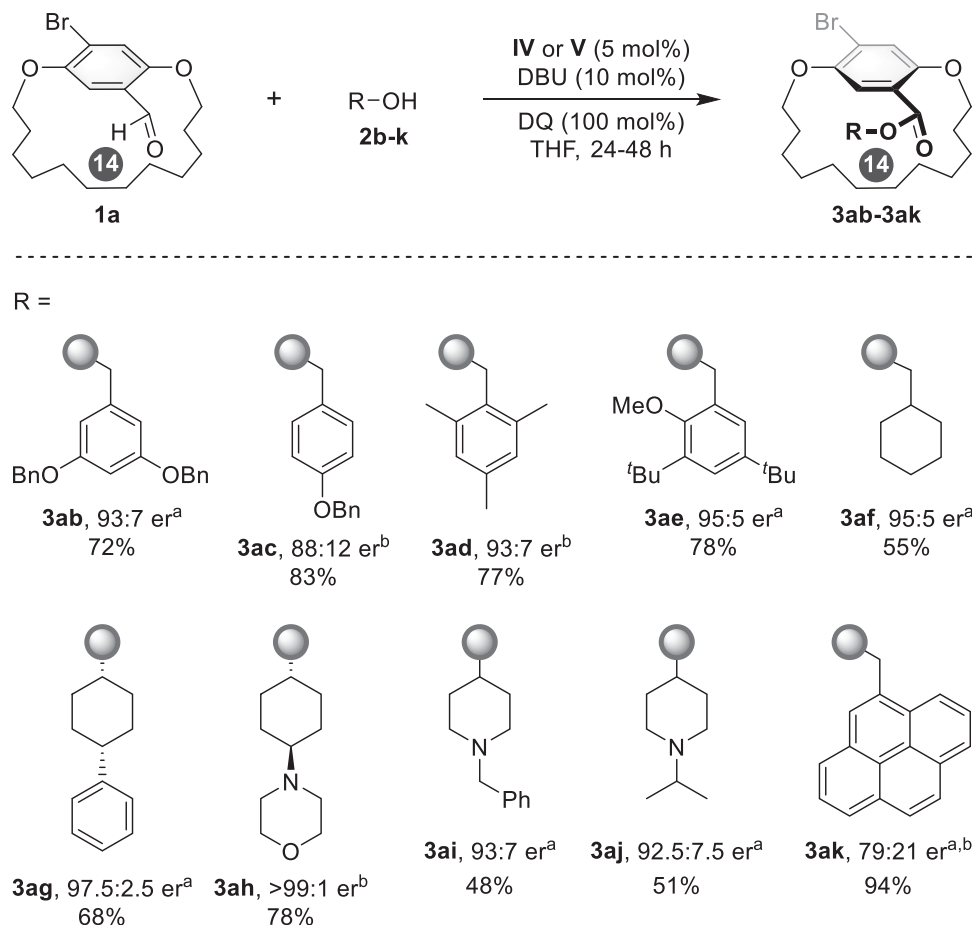


Fig. 3 | Evaluation of the effect of various alcohol substrates. ^aThe reaction was performed at room temperature, **IV** was used as catalyst. ^bThe reaction was performed at 40 °C, **V** was used as catalyst.

but low enantioselectivity, while amino alcohol-derived chiral NHC **VII** afforded the desired product in good yield with moderate enantioselectivity (entries 2, 3, and 6). The N-substituents of the indanol-derived catalysts have an obvious impact on the enantioselectivity of the reaction, as N-2,4,6-(Me)₃C₆H₂ (Mes), N-2,4,6-(Br)₃C₆H₂, or N-C₆F₅ substituents gave the product in high yield but with poor enantioselectivity (entries 2, 3, and 6). Pleasingly, the enantioselectivity was dramatically increased when bulky N-2,4,6-(Pr)₃C₆H₂ or N-2,4,6-Cy₃C₆H₂⁵¹ substituted indanol-derived NHC **IV** or **V** catalyst was used (entry 4–5, 93:7 er). Further base optimization indicated that strong bases, such as DBU and Cs₂CO₃, resulted in higher yields compared to relatively weak bases (entries 8–10). Subsequent solvent experimentation demonstrated that THF achieved the highest yields (entries 11–13). Decreasing the catalyst loading was not detrimental to reaction outcomes (entry 14). Interestingly, increase of temperature yielded the product in a higher er (entry 15). The improved enantioselectivity might arise from a faster racemization rate of the substrate, which facilitate the DKR process. The absolute configuration of **3aa** was unambiguously determined by X-ray diffraction analysis of its derivative (*vide infra*).

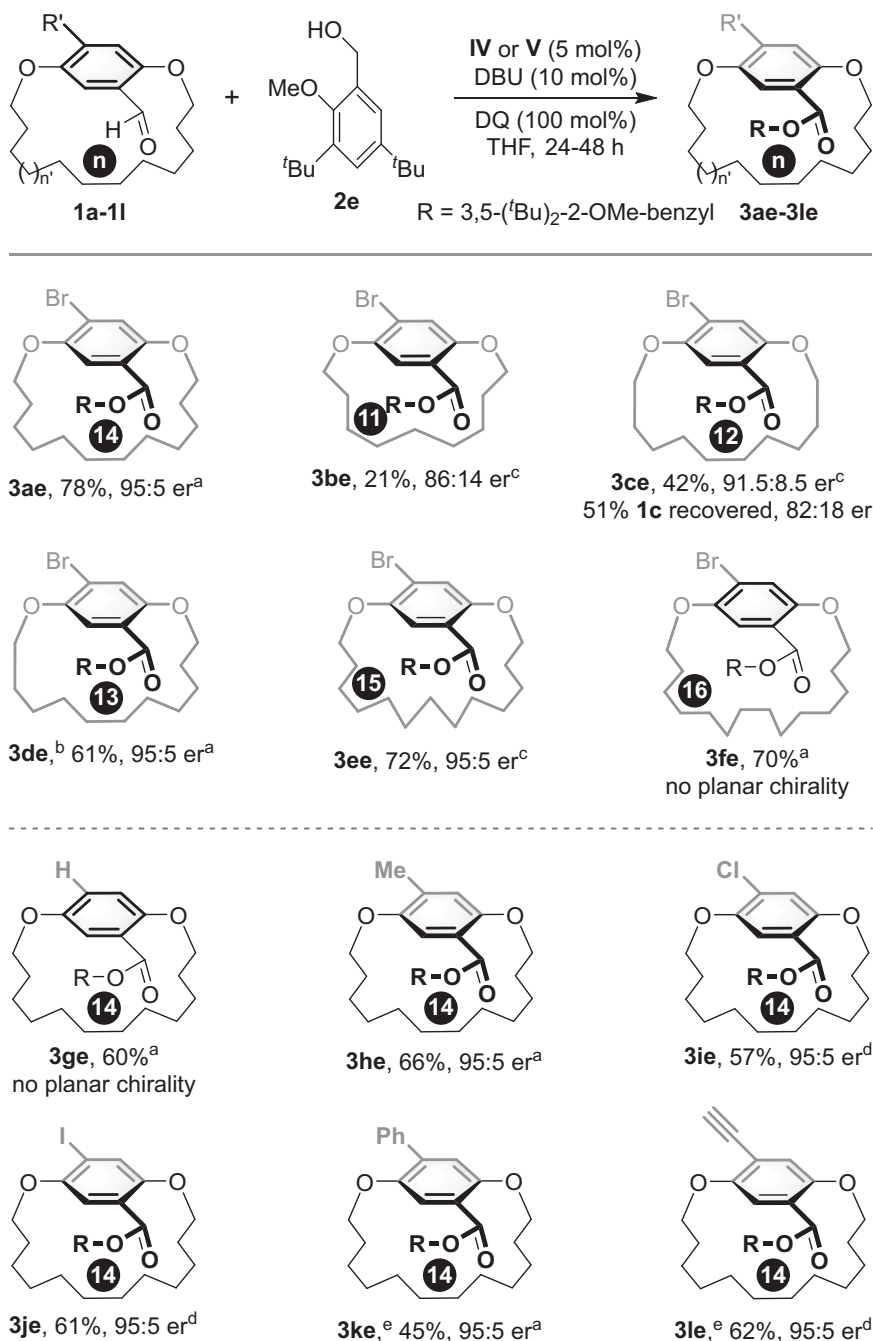
Substrate scope

With the optimized conditions in hand, we then evaluated the effect of the alcohol, starting with substituents on the phenyl ring of the benzyl alcohol. Regardless of the steric and electronics of the aromatic ring substituents, the desired planar-chiral cyclophanes (**3ab–3ad**) were afforded good yield with moderate to good enantioselectivities (Fig. 3). When substrates bearing bulkier groups were used, good yields and high enantioselectivities were achieved (**3ae**, 78% yield and

95:5 er). When other cyclic secondary alcohols were evaluated, the corresponding products **3af–3aj** were obtained in 48–78% yield with er ranging from 93:7 – >99:1. Moreover, the benzyl alcohol with a 4-prenyl group was not an appropriate substrate for this reaction under the optimized conditions (**3ak**).

The investigation of *ansa* chain length and substituent size was conducted using **2e** as model substrate (Fig. 4). Reducing to 11- or 12-membered *ansa* chains, the reaction went through a kinetic resolution process, in which planar-chiral products **3be** and **3ce** were obtained in 86:14 er and 91.5:8.5 er, respectively, while **1c** was recovered with 51% yield and 82:18 er. Using a 13-membered *ansa* chain was feasible, delivering the planar-chiral [13]paracyclophane **3de** with moderate yield and good enantioselectivity. Increasing the *ansa* chain length and using a 15-membered compound was tolerated and gave the product **3ee** in 72% yield with a 95:5 er value, while [16]paracyclophane **3fe** led to the loss of planar chirality due to the relative low rotation barrier.

In addition, an examination of the aromatic ring substituent size was performed (Fig. 4). 4-H substituted [14]paracyclophane resulted in the loss of planar chirality (**3ge**), but [14]paracyclophanes bearing chloro, methyl, or iodo groups on the benzene ring allowed the NHC-catalyzed DKR to occur, generating the planar-chiral cyclophanes in good yields and enantioselectivities (**3he–3je**). Installment of phenyl or ethynyl groups on the aromatic ring was also tolerated. The products **3ke** and **3le** were obtained in high er value, and corresponding substrates **2k** and **2l** were recovered in low er value, which suggested racemization of the substrates occurred. These results indicate that the DKR of planar-chiral [n]paracyclophanes is highly dependent on *ansa* chain length and the size of substituents in the aromatic ring,

**Fig. 4 | Evaluation of the ansa chain length and aromatic ring substituent size.**

^aThe reaction was performed at room temperature, **IV** was used as catalyst. ^bThe reaction was performed at 40 °C, **V** was used as catalyst. ^c0.2 mmol of **2a** was used.

^dThe reaction was performed at 50 °C, **V** was used as catalyst. ^eThe reaction was stirred at room temperature for 24 h, **1k** was recovered in 55:45 er, and **1l** was recovered in 50:50 er.

which allows substrate racemization but limits bond flip in the product's aromatic ring.

Encouraged by these results, we continued to explore the scope of [n]paracyclophanes in this NHC-catalyzed DKR reaction. A diverse array of achiral paracyclophanes with a variety of ansa chain lengths and substituents were tested (Fig. 5). [13]paracyclophane with a chloro group at the 4-position of the phenyl ring performed well to deliver the corresponding planar chiral product (**3ae**) in good yield and enantioselectivity. [14] and [15]paracyclophanes bearing different substituents (vinyl, iodo, ethynyl, phenyl) at the phenyl ring were also accommodated and provided the enantioenriched products (**3be-3fe**). Heteroaromatic rings like 3-thienyl could be introduced at the 4-position of the substrates (**3ge**, **3he**). [16] and [17]paracyclophane with 2-naphthyl,

benzofuran-6-yl or benzo[b]thiophen-3-yl yielded the products in high enantioselectivity (**3ie-3ke**), as could [18]paracyclophane with benzofuran-6-yl albeit with lower enantioselectivity (**3le**). In addition, modifications of the ansa chain were also investigated. The yield of [14] and [15]paracyclophane with an ester group or nitrogen-linked ansa chain decreased to 26% and 16% (**3me**, **3ne**), respectively. The decreased yield of **3me** probably originated from substrate decomposition under the reaction conditions. [15]paracyclophane with an oxygen-linked ansa chain afforded the product in good yield with high enantioselectivity (**3oe**). To assess the configurational stability of the planar-chiral products, **3ae** in toluene was heated to 110 °C. Notably, HPLC analysis indicated that no racemization of **3ae** was observed, even after 7 days at this temperature (see Supplementary Information).

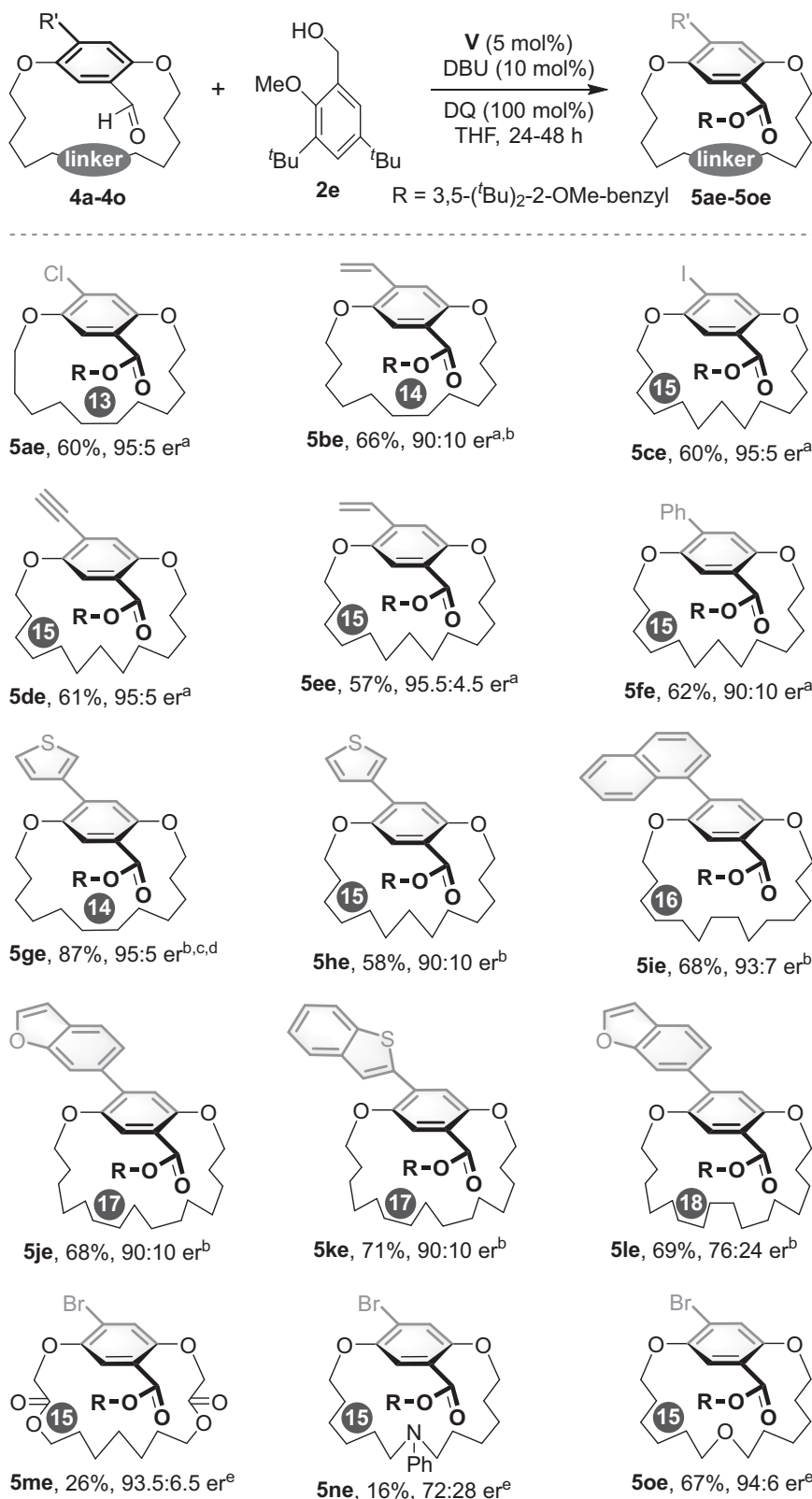


Fig. 5 | The scope of [n]paracyclophanes. ^aThe reaction was performed at 40 °C. ^bThe reaction was performed at 50 °C. ^cThe reaction was performed at room temperature. **5ge** was obtained in 86:14 er. ^dThe reaction was performed at 40 °C, **5ge** was obtained in 92:8 er. ^eThe reaction was performed at 40 °C, **IV** was used as catalyst.

To expand the potential utility of this process, we further manipulated the planar-chiral cyclophane (Fig. 6A). The ester in **3ae** could be reduced with LiAlH₄ to generate benzylic alcohol **6** in 98% yield with only a slight erosion of enantioselectivity. In addition, a Ni-

catalyzed cross-coupling reaction of **3ae** with diphenylphosphine afforded planar-chiral phosphine **7** in 61% yield with a slight loss of stereochemical integrity due to the vigorous reaction conditions. Moreover, the enantiomerically enriched triazole **8** was obtained by a

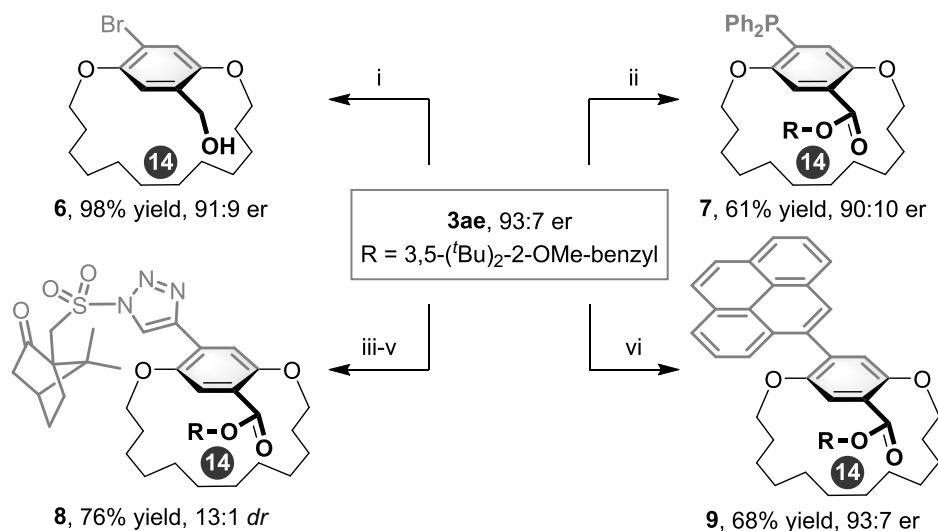
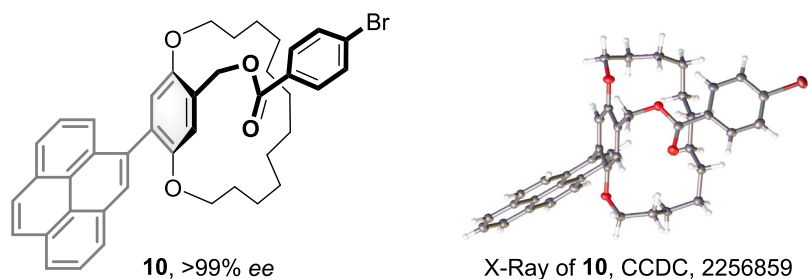
A Synthetic transformation of enantioenriched [14]paracyclophane **3ae**.**B** X-ray of planar-chiral cyclophane **10**.

Fig. 6 | Derivatizations of the chiral product. **A** Synthetic transformation of enantioenriched [14]paracyclophane **3ae**. Reaction conditions: (i) LiAlH₄, 0 °C, THF, 2 h. (ii) Ni(dppe)Cl₂, Ph₂PH, Et₃N, DMF, 120 °C, 12 h. (iii) Pd(PPh₃)₂Cl₂, CuI, TMS-acetylene, Et₃N, 50 °C, 10 h, THF, 91% yield, 93:7 er. (iv) TBAF·3H₂O, THF, rt,

4 h, 87% yield, 93:7 er. (v) CuTC, (*R*)-Camphor-10-sulfonyl azide, toluene, rt, 4 h, 96% yield, 13:1 *dr*. (vi) Pd(PPh₃)₄, Na₂CO₃, pyren-1-ylboronic acid, 1,4-dioxane, 100 °C, 24 h, 68% yield, 93:7 er. **B** X-ray of planar-chiral cyclophane **10**.

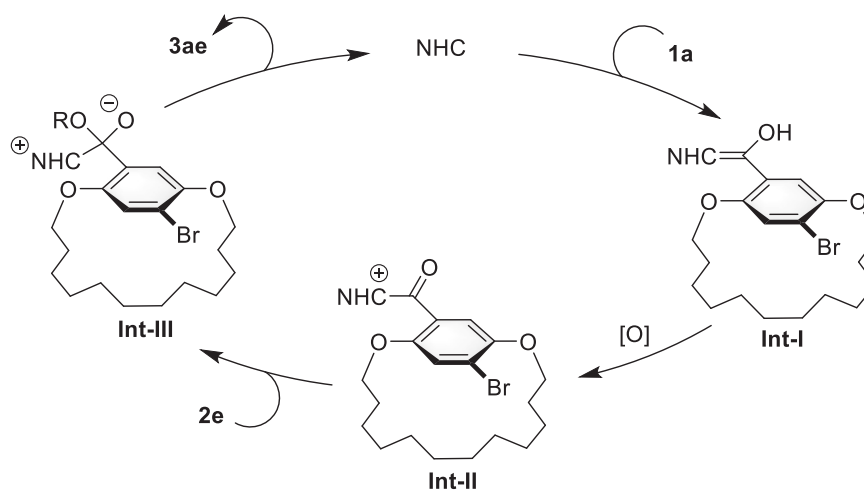


Fig. 7 | Postulated mechanism of the reaction.

Sonogashira cross-coupling, desilylation, and CuTC-catalyzed click reaction sequence. Finally, **3ae** was easily transferred to corresponding pyrene-bearing product **9** in 68% yield and 93:7 er through a Suzuki–Miyara cross-coupling reaction with pyren-1-ylboronic acid. The absolute configuration of **10** was unambiguously determined by

X-ray diffraction analysis (https://www.ccdc.cam.ac.uk/data_request/cif) (Fig. 6B).

A postulated mechanism is illustrated in Fig. 7. The reaction starts from the addition of NHC catalyst **IV** to aldehyde **1a** to generate Breslow intermediate **Int-I**. Then, the oxidation of **Int-I** forms acylazolium

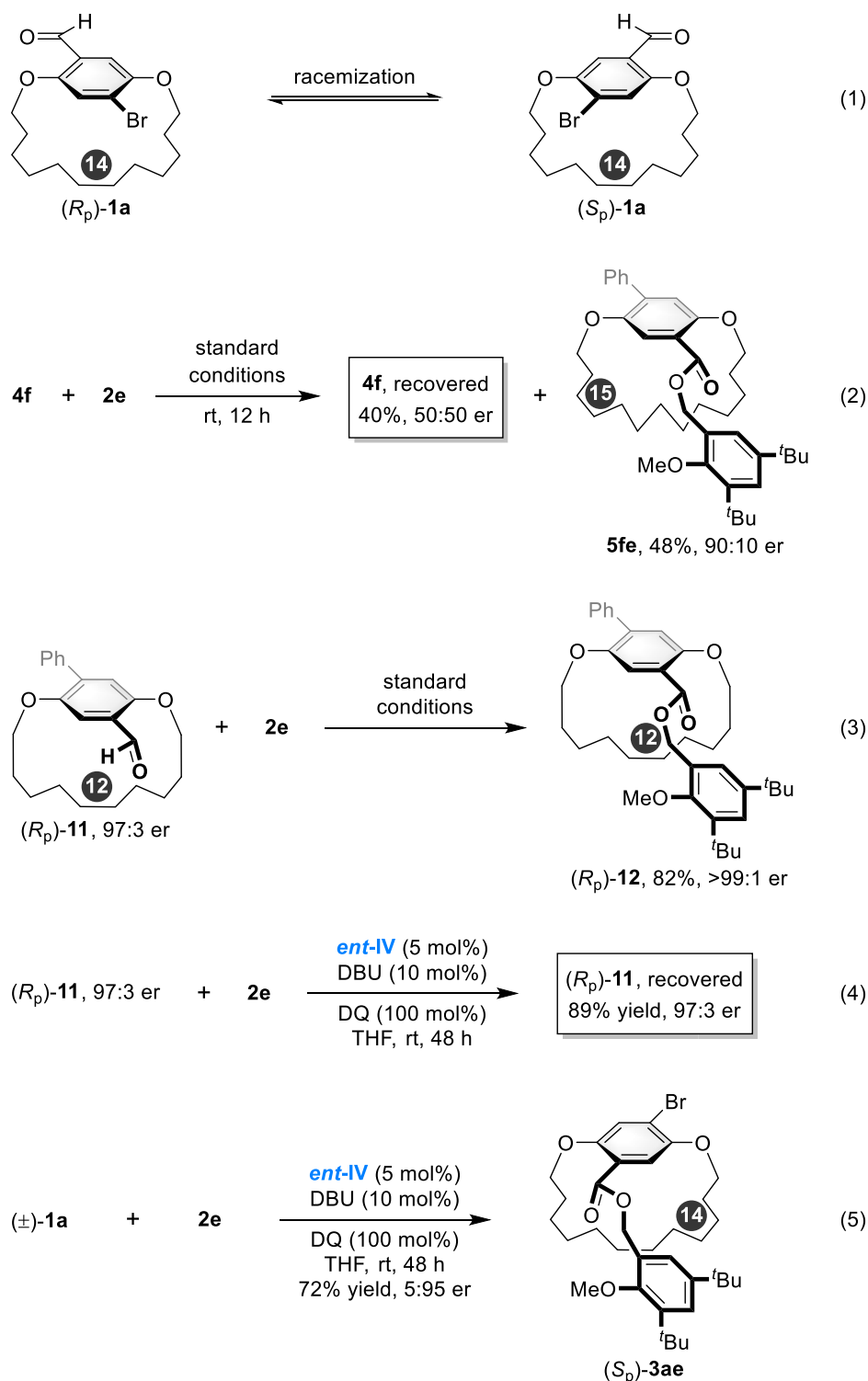


Fig. 8 | Controlled experiments of the dynamic kinetic resolution process.

intermediate **Int-II**. Finally, the esterification of **Int-II** with benzylic alcohol **2e** delivers the planar-chiral product **3ae** and releases the free NHC catalyst **IV**.

The DKR process originates from the rapid bond flip of the aromatic ring in the two enantiomers ($[S_p]$ -**1a** and $[R_p]$ -**1a**) and the reaction-rate difference with the addition of NHC catalyst (Fig. 8, eq 1). To clarify the DKR process, several controlled experiments were conducted. The reaction of [15]paracyclophane **4f** with **2e** was performed under standard conditions for 12 h; **5fe** was obtained in 48% yield with

90:10 er, and **4f** was recovered as racemates in 40% yield. The result indicates that the racemization of **4k** is rapid and not the rate-determined step (Fig. 8, eq 2). In addition, as illustrated in the investigation of substrate scope, [12]paracyclophane underwent kinetic resolution, thus, enantioenriched 4-phenyl-substituted [12]paracyclophane (R_p) -**11** was treated under the optimized reaction conditions, the reaction proceeds smoothly to deliver (R_p) -**12** in 82% yield with >99:1 er value (Fig. 8, eq 3). Alternatively, only a trace amount of (R_p) -**12** was obtained by using **ent-IV** as NHC catalyst (<5% yield), and

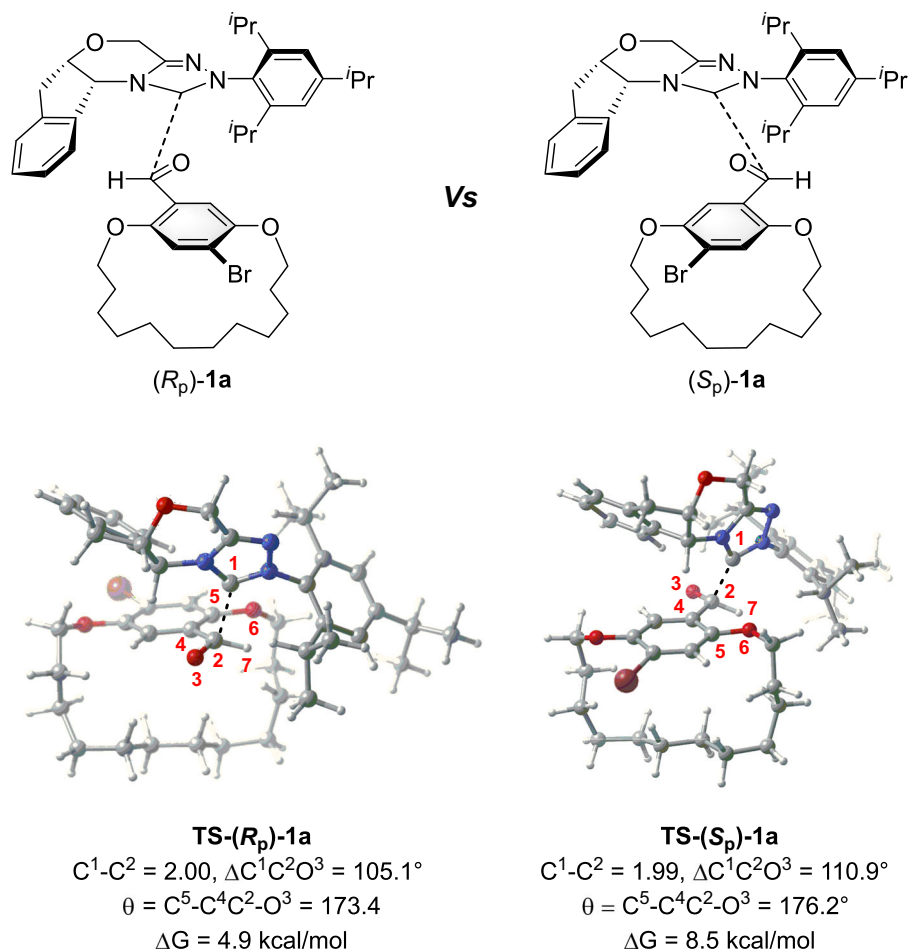


Fig. 9 | Calculated energy profile. Calculated energy profile of the addition of NHC catalyst **IV** to [14]paracyclophane **1a**.

the (*R_p*)-**11** was recovered in 89% yield with 97:3 er value (Fig. 8, eq 4). Further, the reaction of **1a** and **2e** with *ent*-**IV** as catalyst gave a reverse selectivity, suggesting that the (*R_p*)-**11** was unmatched with *ent*-**IV** (Fig. 8, eq 5). These results indicate that the reaction of NHC catalyst **IV** to (*R_p*)-**11** is kinetically favored.

To further explore the energy-difference for the addition of NHC catalyst **IV** to the enantiomers (*S_p*)-**1a** and (*R_p*)-**1a**, a density functional theory (DFT) study was performed using Gaussian 09. As illustrated in Fig. 9, the energy barrier of the addition of NHC catalyst **IV** to (*R_p*)-**1a** is 3.6 kcal/mol lower than that of (*S_p*)-**1a**; thus, the addition of NHC catalyst **IV** to (*R_p*)-**1a** is kinetically favored. Further analysis of transition states **TS-(*S_p*)-1a** and **TS-(*R_p*)-1a** using atoms-in-molecules^{52,53} and noncovalent interactions analyses⁵⁴ reveal that the weak interactions in **TS-(*R_p*)-1a** are stronger than those observed in **TS-(*S_p*)-1a**, which leads to **TS-(*R_p*)-1a** having a lower energy barrier. Interactions in **TS-(*R_p*)-1a** include: seven C–H... π interactions, four C–H...O hydrogen bond interactions, two C–H...N hydrogen bond interactions, one Lp... π interaction, one C–H...Br halogen bond interaction, and ten C–H...H–C van der Waals interactions. Interactions in **TS-(*S_p*)-1a** include: four C–H... π interactions, three C–H...O hydrogen bond interactions, one C–H...N hydrogen bond interaction, two C–H...Br halogen bond interactions, and nine C–H...H–C van der Waals (See Supplementary Fig. 2). Although the calculated results are consistent with the observed experiments, a relatively low Gibbs free energy for addition of NHC catalyst to the substrate suggests a rapid rate for this transformation. While the subsequent oxidative esterification is not the enantioselectivity-determined step, together with experimental observation that increases the reaction temperature led to a higher

enantioselectivity. Thus, the Curtin-Hammett scenario might be operative for the DKR approach⁵⁵.

Discussion

In summary, we developed an NHC-catalyzed enantioselective synthesis of planar-chiral cyclophanes. The reaction features a DKR process involving an aldehyde oxidation esterification and affords a wide range of planar-chiral macrocycles in good to high yields with high enantioselectivities. An investigation of *ansa* chain length and the size of aromatic ring substituents indicated that these variables were crucial to generating the planar chirality. Further, the cyclophane products could be transformed into other planar-chiral macrocyclic scaffolds by simple reactions. Controlled experiments and DFT calculations were performed to clarify the DKR process. An application of these planar-chiral scaffolds for library inclusion and asymmetric catalysis are under investigation in our lab.

Methods

Materials. For ¹H NMR, ¹³C NMR, and high-performance liquid chromatography spectra of compounds in this manuscript, see Supplementary Figures. For details of the synthetic macrocycle substrates: diphenol (10.0 mmol) and dibromides (10.0 mmol) in DMF (25.0 mL) were slowly added to a suspension of K₂CO₃ (3.45 g, 25.0 mmol) and NaI (170 mg, 1.0 mmol) in DMF (150 mL) at 140 °C over 18 h. The solvent was removed under reduced pressure. The aqueous phase was extracted with EtOAc (3 × 50 mL), and the combined organic layers were washed with water and brine, and dried over Na₂SO₄. The solvent was removed under reduced pressure, and the residue was purified by

flash column chromatography on silica gel affording the products (yield: 10–40%).

Synthesis of **3** and **5**. To a 15 mL Schlenk tube equipped with a magnetic stirring bar was added macrocycles substrates **1** or **4** (0.10 mmol), **2** (0.4 mmol), NHC precursor **IV** or **V** (0.005 mmol), DBU (0.01 mmol) and DQ (0.1 mmol). The tube was closed with a septum, evacuated, and refilled with nitrogen (3 cycles). Then, freshly distilled THF (1.0 mL) was added to the reaction mixture and stirred for 10–72 h. Upon completion (monitored by TLC), the solvent was evaporated, and the residue was purified by silica gel column chromatography to afford the planar-chiral cyclophanes **3** or **5**.

Reporting summary

Further information on research design is available in the Nature Portfolio Reporting Summary linked to this article.

Data availability

The authors declare that the data supporting the findings of this study are available within the article and Supplementary Information file, or from the corresponding author upon request. The X-ray crystallographic coordinates for structures reported in this study have been deposited at the Cambridge Crystallographic Data Centre (CCDC), under deposition numbers CCDC 2256859 (for (**R_p**)-**10**). These data can be obtained free of charge from The Cambridge Crystallographic Data Centre via www.ccdc.cam.ac.uk/data_request/cif. The full experimental details for the preparation of all new compounds, and their spectroscopic and chromatographic data generated in this study are provided in the Supplementary Information/Source Data file. All data are available from the authors upon request. Source data are provided with this paper.

References

- Ciardello, J. J., Stewart, H. L., Sore, H. F., Galloway, W. R. J. D. & Spring, D. R. A novel complexity-to-diversity strategy for the diversity-oriented synthesis of structurally diverse and complex macrocycles from quinine. *Bioorg. Med. Chem.* **25**, 2825–2843 (2017).
- Driggers, E. M., Hale, S. P., Lee, J. & Terrett, N. K. The exploration of macrocycles for drug discovery—an underexploited structural class. *Nat. Rev. Drug Discov.* **7**, 608–624 (2008).
- Lau, Y. H. et al. Double strain-promoted macrocyclization for the rapid selection of cell-active stapled peptides. *Angew. Chem. Int. Ed.* **54**, 15410–15413 (2015).
- Syed, Y. Y. Lorlatinib: first global approval. *Drugs* **79**, 93–98 (2019).
- Vögtle, F. & Neumann, P. Zur nomenklatur der phane. *Tetrahedron Lett.* **10**, 5329–5334 (1969).
- Cram, D. J. & Cram, J. M. Cyclophane chemistry: bent and battered benzene rings. *Acc. Chem. Res.* **4**, 204–213 (1971).
- Tobe, Y. & Sonoda, M. In *Modern Cyclophane Chemistry*, 1–40 (Wiley-VCH, Weinheim, 2004).
- Marshall, J. A. Trans-cycloalkenes and [a.b]betweenanenes, molecular jump ropes and double bond sandwiches. *Chem. Soc. Rev.* **11**, 213–218 (1980).
- Liu, Z. C., Nalluri, S. K. M. & Stoddart, J. F. Surveying macrocyclic chemistry: from flexible crown ethers to rigid cyclophanes. *Chem. Soc. Rev.* **46**, 2459–2478 (2017).
- Tanaka, K. Catalytic enantioselective synthesis of planar chiral cyclophanes. *Bull. Chem. Soc. Jpn.* **91**, 187–194 (2018).
- Gulder, T. & Baran, P. S. Strained cyclophane natural products: macrocyclization at its limits. *Nat. Prod. Rep.* **29**, 899–934 (2012).
- Romero, D. Benefit with daratumumab maintenance. *Nat. Rev. Clin. Oncol.* **18**, 676 (2021).
- Zahid, H., Eduard, S., Knoll, D. M., Joerg, L. & Stefan, B. Planar chiral [2.2] paracyclophanes: from synthetic curiosity to applications in asymmetric synthesis and materials. *Chem. Soc. Rev.* **47**, 6947–6963 (2018).
- Ramaiah, D., Neelakandan, P. P., Nair, A. K. & Avirah, R. R. Functional cyclophanes: promising hosts for optical biomolecular recognition. *Chem. Soc. Rev.* **42**, 4158–4168 (2010).
- Sambasivarao, K., Eknath, S. M. & Waghule, G. T. Selected synthetic strategies to cyclophanes. *Beilstein J. Org. Chem.* **11**, 1274–1331 (2015).
- López, R. & Palomo, C. Planar chirality: a mine for catalysis and structure discovery. *Angew. Chem. Int. Ed.* **61**, e202113504b (2022).
- Kanomata, N. & Nakata, T. A compact chemical miniature of a holoenzyme, coenzyme nadh linked dehydrogenase. Design and synthesis of bridged nadh models and their highly enantioselective reduction. *J. Am. Chem. Soc.* **122**, 4563–4568 (2000).
- Kanomata, N. & Ochiai, Y. Stereocontrol of molecular jump-rope: crystallization-induced asymmetric transformation of planar-chiral cyclophanes. *Tetrahedron Lett.* **42**, 1045–1048 (2001).
- Kanomata, N. & Oikawa, J. Adsorption-induced asymmetric transformation of planar-chiral pyridinophanes. *Tetrahedron Lett.* **44**, 3625–3628 (2003).
- Yoshida, Y., Kanashima, Y., Mino, T. & Sakamoto, M. Asymmetric syntheses and applications of planar chiral hypervalent iodine(v) reagents with crown ether backbones. *Tetrahedron* **75**, 3840–3849 (2019).
- Ueda, T., Kanomata, N. & Machida, H. Synthesis of planar-chiral paracyclophanes via samarium(II)-catalyzed intramolecular pinacol coupling. *Org. Lett.* **7**, 2365–2368 (2005).
- Tanaka, K., Sagae, H., Toyoda, K., Noguchi, K. & Hirano, M. Enantioselective syn planar chiral metacyclophane through Rh-cat alkyne cyclotrimerization [a,w-diyne rxn DMAD to bicyclic phthalate]. *J. Am. Chem. Soc.* **129**, 1522–1523 (2007).
- Tanaka, K., Sagae, H., Toyoda, K. & Hirano, M. Enantioselective synthesis of planar-chiral metacyclophanes through cationic Rh(I)/modified-BINAP-catalyzed inter- and intramolecular alkyne cyclotrimerizations. *Tetrahedron* **64**, 831–846 (2008).
- Araki, T., Noguchi, K. & Tanaka, K. Enantioselective synthesis of planar-chiral garba-paracyclophanes: rhodium-catalyzed [2 + 2 + 2] cycloaddition of cyclic diynes with terminal monoynes. *Angew. Chem. Int. Ed.* **52**, 5617–5621 (2013).
- Nogami, J. et al. Enantioselective synthesis of planar chiral zigzag-type cyclophenylene belts by rhodium-catalyzed alkyne cyclotrimerization. *J. Am. Chem. Soc.* **142**, 9834–9842 (2020).
- Tanaka, K., Hori, T., Osaka, T., Noguchi, K. & Hirano, M. Rhodium-catalyzed reactions of dithiols and 1,4-bis(bromomethyl)benzenes leading to enantioenriched dithiaparacyclophanes. *Org. Lett.* **9**, 4881–4884 (2007).
- Ding, Q., Wang, Q., He, H. & Cai, Q. Asymmetric synthesis of (–)-pterocarine and (–)-galeon via chiral phase transfer-catalyzed atropselective formation of diarylether cyclophane skeleton. *Org. Lett.* **19**, 1804–1807 (2017).
- Gagnon, C. et al. Biocatalytic synthesis of planar chiral macrocycles. *Science* **367**, 917–921 (2020).
- Yu, S., Shen, G., He, F. & Yang, X. Asymmetric synthesis of planar-chiral macrocycles via organocatalyzed enantioselective macrocyclization. *Chem. Commun.* **58**, 7293–7296 (2022).
- Wei, S., Chen, L.-Y. & Li, J. Enantioselective synthesis of planar chiral macrocyclic metacyclophanes by Pd-catalyzed C–O cross-coupling. *ACS Catal.* **13**, 7450–7456 (2023).
- Tan, L., Sun, M., Wang, H., Kim, J. & Lee, M. Enantiocontrolled macrocyclization by encapsulation of substrates in chiral capsules. *Nat. Synth.* **2**, 1222–1231 (2023).
- Yang, G., He, Y., Wang, T., Li, Z. & Wang, J. Atroposelective synthesis of planar-chiral indoles via carbene catalyzed macrocyclization. *Angew. Chem. Int. Ed.* **63**, e202316739 (2024).

33. Kanda, K., Endo, K. & Shibata, T. Enantioselective synthesis of planar-chiral 1, n-dioxal[n]paracyclophanes via catalytic asymmetric ortho-lithiation. *Org. Lett.* **12**, 1980–1983 (2010).
34. Kanda, K., Koike, T., Endo, K. & Shibata, T. The first asymmetric sonogashira coupling for the enantioselective generation of planar chirality in paracyclophanes. *Chem. Commun.* **14**, 1870–1872 (2009).
35. Wang, D., Shao, Y.-B., Chen, Y., Xue, X.-S. & Yang, X. Y. Enantioselective synthesis of planar-chiral macrocycles through asymmetric electrophilic aromatic amination. *Angew. Chem. Int. Ed.* **61**, e202201064 (2022).
36. Nair, V. et al. Employing homoenolates generated by NHC catalysis in carbon–carbon bond-forming reactions: state of the art. *Chem. Soc. Rev.* **40**, 5336–5346 (2011).
37. Biju, A. T., Kuhl, N. & Glorius, F. Extending NHC-catalysis: coupling aldehydes with unconventional reaction partners. *Acc. Chem. Res.* **44**, 1182–1195 (2011).
38. Bugaut, X. & Glorius, F. Organocatalytic umpolung: N-heterocyclic carbenes and beyond. *Chem. Soc. Rev.* **41**, 3511–3522 (2012).
39. Ryan, S. J., Candish, L. & Lupton, D. W. Cheminform abstract: acyl anion free N-heterocyclic carbene organocatalysis. *Chem. Soc. Rev.* **42**, 4906–4917 (2013).
40. Mahatthananchai, J. & Bode, J. W. On the mechanism of N-heterocyclic carbene-catalyzed reactions involving acyl azoliums. *Acc. Chem. Res.* **47**, 696–707 (2014).
41. Hopkinson, M. N., Richter, C., Schedler, M. & Glorius, F. An overview of N-heterocyclic carbenes. *Nature* **510**, 485–496 (2014).
42. Ishii, T., Nagao, K. & Ohmiya, H. Recent advances in N-heterocyclic carbene-based radical catalysis. *Chem. Sci.* **11**, 5630–5636 (2020).
43. Chen, X.-K., Wang, H.-L., Jin, Z.-C. & Chi, Y. R. N-heterocyclic carbene organocatalysis: activation modes and typical reactive intermediates. *Chin. J. Chem.* **38**, 1167–1202 (2020).
44. Chen, X.-Y., Cao, Z.-H. & Ye, S. Bifunctional N-heterocyclic carbenes derived from *i*-pyroglutamic acid and their applications in enantioselective organocatalysis. *Acc. Chem. Res.* **53**, 690–702 (2020).
45. Feng, J. & Du, D. Asymmetric synthesis of atropisomers enabled by N-heterocyclic carbene catalysis. *Tetrahedron* **100**, 132456 (2021).
46. Song, R., Xie, Y., Jin, Y. & Chi, Y. R. Carbene-catalyzed asymmetric construction of atropisomers. *Angew. Chem. Int. Ed.* **60**, 26026–26037 (2021).
47. Wang, J. M., Zhao, C. G. & Wang, J. Recent progress toward the construction of axially chiral molecules catalyzed by an N-heterocyclic carbene. *ACS Catal.* **11**, 12520–12531 (2021).
48. Lu, S., Poh, S. B. & Zhao, Y. Kinetic resolution of 1,1'-biaryl-2,2'-diols and amino alcohols through NHC-catalyzed atroposelective acylation. *Angew. Chem. Int. Ed.* **46**, 11041–11045 (2015).
49. Zhao, C. G. et al. Enantioselective [3 + 3] atroposelective annulation catalyzed by N-heterocyclic carbenes. *Nat. Commun.* **9**, 611 (2018).
50. Lv, X. K. et al. Access to planar chiral ferrocenes via N-heterocyclic carbene-catalyzed enantioselective dsymmetrization reactions. *ACS Catal.* **12**, 2706–2713 (2022).
51. Yan, J.-L. et al. Carbene-catalyzed atroposelective synthesis of axially chiral styrenes. *Nat. Commun.* **13**, 84 (2022).
52. McLean, A. & Chandler, D. G. S. Contracted gaussian basis sets for molecular calculations. I. second row atoms, Z = 11–18. *J. Chem. Phys.* **72**, 5639–5648 (1980).
53. Raghavachari, K., Binkley, J. S., Seeger, R. & Pople, J. A. Self-consistent molecular orbital methods. XX. A basis set for correlated wave functions. *J. Chem. Phys.* **72**, 650–654 (1980).
54. Bader, R. F. W. Atoms in molecules. *Acc. Chem. Res.* **18**, 9–15 (1985).
55. Seeman, J. I. Effect of conformational change on reactivity in organic chemistry. evaluations, applications and extensions of Curtin–Hammett Winstein–Holness kinetics. *Chem. Rev.* **83**, 83–134 (1983).

Acknowledgements

This project was financially supported by the National Natural Science Foundation of China (No. 22171027, 22103005), the Beijing Natural Science Foundation (No. 2212009), the Fundamental Research Funds for the Central Universities (No. 2233300007) and the High Performance Computing Platform of Beijing University of Chemical Technology (BUCT). We thank Prof. Dr. Guofu Zi (Beijing Normal University) for the X-ray diffraction analysis and Dr. Stephanie A. Blaszczyk for proofread the manuscript (Moxie Medical Writing).

Author contributions

J.Y.L. conducted main experiments; Z.Y.D. prepared several starting materials; X.E.Y. optimized the reaction conditions and prepared several starting materials during the revision of the manuscript. Y.C. and Z.H.Y. performed part of the DFT computation; M.W. and C.Y.L. rerun the computation during the revision of the manuscript. C.G.Z. conceptualized and directed the project, and drafted the manuscript with the assistance from co-authors. All authors contributed to discussions.

Competing interests

The authors declare no competing interests.

Reprints and permission information is available online at <http://npg.nature.com/reprintsandpermissions/>

Additional information

Supplementary information The online version contains supplementary material available at <https://doi.org/10.1038/s41467-024-46376-8>.

Correspondence and requests for materials should be addressed to Chenyang Li or Changgui Zhao.

Peer review information *Nature Communications* thanks the anonymous reviewers for their contribution to the peer review of this work. A peer review file is available.

Reprints and permissions information is available at <http://www.nature.com/reprints>

Publisher's note Springer Nature remains neutral with regard to jurisdictional claims in published maps and institutional affiliations.

Open Access This article is licensed under a Creative Commons Attribution 4.0 International License, which permits use, sharing, adaptation, distribution and reproduction in any medium or format, as long as you give appropriate credit to the original author(s) and the source, provide a link to the Creative Commons licence, and indicate if changes were made. The images or other third party material in this article are included in the article's Creative Commons licence, unless indicated otherwise in a credit line to the material. If material is not included in the article's Creative Commons licence and your intended use is not permitted by statutory regulation or exceeds the permitted use, you will need to obtain permission directly from the copyright holder. To view a copy of this licence, visit <http://creativecommons.org/licenses/by/4.0/>.

© The Author(s) 2024